

Integrated Phyto-Bio-Synthetic Matrix for Self-Healing Bio-Concrete: Performance and Durability Evaluation

Pearlin C.P¹, Sheena A.D^{2*}

¹ Department of Civil Engineering, Vels Institute of Science, Technology & Advanced Studies (VISTAS), India - 600117. Email: cppearlin@gmail.com

^{2*} Department of Civil Engineering, Vels Institute of Science, Technology & Advanced Studies (VISTAS), India - 600117. (Corresponding Author) Email: dr.sheenaad@gmail.com

*Corresponding Author: Dr. A.D. Sheena, Email: dr.sheenaad@gmail.com

Received: 20th Feb, 2026 | Revised: 4th Mar, 2026 | Accepted: 25th Mar, 2026 | Available Online: 10th Apr, 2026

ABSTRACT

Cracks in concrete make it easier for chloride ions to enter, which accelerates corrosion of the reinforcement and reduces durability. Traditional repair methods are often expensive and increase carbon emissions. In this study, we introduce a self-healing concrete that uses an Integrated Phyto-Bio-Synthetic (IPBS) matrix. This matrix combines pozzolanic densification, fiber-controlled crack regulation, and microbial calcite precipitation. Rice husk ash serves as both a supplementary cement material and a carrier for microbes. Pre-treated bamboo fibers help bridge cracks, neem and thulasi act as plant-based stabilizers, and *Bacillus subtilis* produces calcite. To determine how effectively the IPBS system works, we conducted compressive, split tensile, and flexural strength tests. We corroborated the findings with permeability indicators and photographs of crack closure during wet-dry curing. Scanning electron microscopy (SEM) and X-ray diffraction (XRD) revealed microstructural details that corroborated these findings. With these improvements, the IPBS mix achieved compressive, split tensile, and flexural strengths that were 20% higher than those of regular concrete. The system also became much more durable: crack-healing efficiency increased from about 5% to 55%, and permeability and chloride ingress dropped significantly. In summary, the IPBS system uses agricultural waste and repairs cracks automatically. This approach improves both strength and durability and helps produce concrete with a lower carbon footprint.

Keywords: Integrated Phyto-Bio-Synthetic matrix; microbial self-healing concrete; rice husk ash; bamboo fiber reinforcement; phytogenic stabilizers; *Bacillus subtilis*; durability and permeability.

How to cite this article: Pearlin CP, Sheena AD. Integrated Phyto-Bio-Synthetic Matrix for Self-Healing Bio-Concrete: Performance and Durability Evaluation. *Int J Drug Deliv Technol.* 2026;16(30s):39-47. DOI: 10.25258/ijddt.16.30s.4

Source of support: Nil.

Conflict of interest: The authors declare no conflict of interest.

INTRODUCTION

Concrete remains the backbone of modern infrastructure due to its versatility, availability, and mechanical robustness; however, its intrinsic susceptibility to cracking continues to undermine long-term durability and structural reliability. Microcracks induced by shrinkage, thermal gradients, mechanical loading, and environmental exposure serve as preferential pathways for moisture and aggressive ions, thereby accelerating reinforcement corrosion and reducing service life. Conventional repair strategies, although effective in the short term, are labor-intensive, economically burdensome, and often fail to address distributed micro-

damage within the material matrix. This limitation has driven the emergence of self-healing concrete systems as a paradigm shift toward autonomous, durable, and low-maintenance infrastructure materials.

Among various self-healing approaches, microbially induced calcium carbonate precipitation (MICP) has gained considerable attention due to its ability to biologically seal cracks through in-situ mineral formation. Bacterial species such as *Bacillus subtilis* are particularly suitable for cementitious environments because of their spore-forming capability and tolerance to high alkalinity. Upon activation by moisture and nutrient availability, these bacteria precipitate calcium

Integrated Phyto-Bio-Synthetic Matrix for Self-Healing Bio-Concrete: Performance and Durability Evaluation

carbonate, which can effectively fill cracks and restore impermeability. Despite its promise, conventional microbial self-healing systems often suffer from limited bacterial survivability, non-uniform distribution, and insufficient crack-width control, thereby restricting their efficiency under real service conditions.

Recent research has explored hybrid strategies combining microbial agents with supplementary cementitious materials and fibers to overcome these challenges. Rice husk ash (RHA), a silica-rich agricultural byproduct, has demonstrated significant potential as a pozzolanic material capable of refining pore structure, enhancing durability, and reducing cement consumption. Moreover, its porous morphology provides a protective microenvironment for bacterial spores, improving their viability over extended periods. Concurrently, natural fibers such as bamboo fibers contribute to crack-width regulation through effective bridging mechanisms, thereby creating favorable conditions for mineral precipitation and crack closure. Controlled crack geometry is particularly critical in microbial healing systems, as excessive crack widths can inhibit effective calcite deposition.

In parallel, the incorporation of phytogenic additives has emerged as a novel approach to stabilize biological activity within cementitious matrices. Herbal compounds derived from neem (*Azadirachta indica*) and thulasi (*Ocimum sanctum*) possess antimicrobial and biochemical regulatory properties that can suppress undesirable microbial growth while maintaining a conducive environment for targeted bacterial activity. However, the interaction between phytogenic additives and beneficial calcite-producing bacteria remains insufficiently understood, particularly in terms of dosage optimization and compatibility within multi-component systems.

LITERATURE REVIEW

Concrete cracking is an unavoidable multi-physics phenomenon arising from restrained shrinkage, thermal gradients, cyclic mechanical loading, and environmental attack, and it becomes a durability driver by creating preferential pathways for water and ion transport. Once cracks form, permeability and effective diffusivity increase nonlinearly with crack width, accelerating chloride ingress and corrosion initiation, thereby shifting the lifecycle burden from embodied carbon to maintenance carbon [1]. Biological self-healing has been positioned as a sustainable alternative because it targets the transport pathway itself—cracks—rather than only

restoring surface integrity, with the additional advantage that mineral precipitation can densify the near-crack microstructure. Foundational demonstrations established that alkali-resistant spore-forming bacteria can be embedded in cementitious matrices and later activated by water to precipitate CaCO_3 as a crack sealant, reducing water permeability and recovering transport performance. [2]

Microbially induced calcium carbonate precipitation (MICP) in cement-based systems is most frequently associated with ureolysis-driven alkalization and carbonate generation, although non-ureolytic pathways—including denitrification and other metabolic routes—can also drive carbonate mineralization depending on substrate availability and local chemistry. Contemporary reviews emphasize that microbial activity is strongly governed by survivability constraints imposed by concrete, including high alkalinity, low internal nutrient availability, and progressive pore refinement that can physically exclude spores or limit metabolite diffusion. These constraints have motivated encapsulation and carrier strategies as essential design components, not ancillary additives. The carrier literature shows that porous phases—ranging from lightweight aggregates to mineral sorbents—can provide sheltered microhabitats and enable more sustained healing responses, in part by buffering local pH and regulating nutrient release. [3]

Hybridization with fibers is a complementary strategy because bacterial healing is crack-width sensitive. Crack closure becomes less efficient as crack width increases due to transport limitations and reduced supersaturation persistence in the crack solution; thus, controlling crack width is mechanistically equivalent to increasing the “healing feasibility window.” Fiber reinforcement acts through crack bridging and distributed microcracking, reducing maximum crack widths and providing nucleation surfaces that can enhance mineral deposition continuity. Recent work explicitly shows that coupling bacteria with fiber reinforcement can elevate mechanical performance while maintaining healing functionality under varied curing conditions, indicating a synergy rather than a trade-off when the system is designed to avoid over-precipitation or nutrient-induced strength loss. [4]

Rice husk ash (RHA) is widely established as a supplementary cementitious material (SCM) with high silica content and a strong potential for pore refinement and permeability reduction through pozzolanic

Integrated Phyto-Bio-Synthetic Matrix for Self-Healing Bio-Concrete: Performance and Durability Evaluation

consumption of portlandite and secondary C–S–H formation. Systematic reviews highlight that RHA performance depends on amorphous silica content, fineness, and optimized replacement level, and multiple analyses support replacement levels commonly in the 10–20% range without compromising strength when processing is controlled. Importantly for bio-concrete, RHA exhibits intrinsic porosity and irregular surface morphology, suggesting a dual role as both a reactive SCM and a micro-reservoir for bacterial spores when appropriately engineered. Direct experimental evidence also indicates that combining RHA with Bacillus-based systems can significantly increase compressive strength and promote self-healing functionality. [5]

Plant-derived additives constitute a less explored dimension in microbial self-healing concrete. While neem and thulasi (holy basil) are well-documented for antimicrobial phytochemicals and bioactive compounds, their incorporation into cementitious systems introduces a compatibility challenge: phytochemicals must suppress deleterious microbial growth and stabilize the system without inhibiting the targeted calcite-producing bacteria. The literature therefore reveals a clear gap: existing studies typically combine two subsystems (bacteria–carrier, bacteria–fiber, or bacteria–SCM), but fully integrated systems that simultaneously co-design biological, phytochemical, fibrous, and pozzolanic components into a single mechanistically coherent IPBS architecture remain scarce, particularly with validated performance and statistically supported outcomes. [6]

METHODOLOGY

The IPBS concept is developed as a coupled transport–reaction–mechanics system whose objective is to reduce crack-driven transport, promote mineral sealing, and maintain or increase load-carrying capacity. The system is composed of four functional subsystems: the pozzolanic matrix modifier (RHA), the fibrous crack kinematics controller (bamboo fibers), the phytochemical stabilizer package (neem and thulasi), and the microbial mineralization agent (*Bacillus subtilis*). The foundational experimental outcomes and baseline performance data used to parameterize the present analytical framework are drawn from the provided manuscript.

□ filecite □ turn0file0 □

Microbial precipitation kinetics are modeled using a reduced-order rate law that captures first-order dependence on active biomass density and nutrient availability. The calcium carbonate precipitation rate is

expressed as:

$$R_{\text{CaCO}_3} = k_p C_b C_{\text{nut}} \quad (1)$$

where R_{CaCO_3} is the precipitation rate of CaCO_3 ($\text{mol}\cdot\text{m}^{-3}\cdot\text{s}^{-1}$), k_p is an effective kinetic coefficient incorporating enzymatic activity and local supersaturation effects, C_b is the concentration of active bacteria ($\text{cells}\cdot\text{m}^{-3}$ or an equivalent biomass proxy), and C_{nut} is the effective nutrient concentration ($\text{mol}\cdot\text{m}^{-3}$) that supports metabolic carbonate generation. This reduced law is consistent with the observation that healing performance is jointly limited by microbial activation and available substrate. For mechanistic completeness, bacterial activation and decay can be approximated by a logistic–decay dynamic:

$$\frac{dC_b}{dt} = \mu C_b \left(1 - \frac{C_b}{C_{b,\text{max}}} \right) - k_d C_b \quad (2)$$

where μ is the specific growth/activation rate, $C_{b,\text{max}}$ is an effective carrying capacity assigned to the porous carrier volume, and k_d represents deactivation/decay under alkaline stress. Carrier-enabled survivability modifies $C_{b,\text{max}}$ and reduces the effective k_d , consistent with carrier-material evidence in cementitious systems. [7]

Crack healing efficiency is quantified using an image-based healed-area ratio defined as:

$$H_c = \frac{A_{\text{healed}}}{A_{\text{initial}}} \times 100 \quad (3)$$

where H_c is crack healing efficiency (%), A_{initial} is the initial crack area (or projected crack void area) at the start of exposure, and A_{healed} is the area filled/closed by mineralization and autogenous products at the evaluation time. Under a crack-filling interpretation, A_{healed} is related to precipitated volume V_p through an effective crack depth d_c such that $A_{\text{healed}} \approx V_p/d_c$, enabling linkages between kinetic precipitation models and observed visual closure. Crack-width sensitivity is incorporated through a transport-limited efficiency function:

Integrated Phyto-Bio-Synthetic Matrix for Self-Healing Bio-Concrete: Performance and Durability Evaluation

$$H_c(w, t) = H_{\max} \left(1 - \exp \left[-\frac{\beta t}{w + w_0} \right] \right) \quad (4)$$

where w is crack width, t is time, H_{\max} is the asymptotic healing capacity for a given system, β aggregates microbial activity and ion transport, and w_0 is a regularization constant reflecting finite transport pathways. This form reflects the widely reported reduction of healing efficiency at larger crack widths and provides a calibration pathway using measured H_c values. [8]

Strength enhancement is treated as the superposition of independent but interacting contributions from pozzolanic densification, fiber bridging, and bio-mineral filling effects:

$$f'_{\text{IPBS}} = f'_{\text{control}} + \Delta f_{\text{pozzolan}} + \Delta f_{\text{fiber}} + \Delta f_{\text{bio}} \quad (5)$$

where f'_{IPBS} and f'_{control} represent the compressive strengths of IPBS and control mixtures, respectively. The pozzolanic contribution is modeled as:

$$\Delta f_{\text{pozzolan}} = \alpha_p \phi_{\text{RHA}} \chi_{\text{Si}} \ln \left(1 + \frac{t}{t_r} \right) \quad (6)$$

where ϕ_{RHA} is the binder replacement fraction by RHA, χ_{Si} is an effective amorphous silica reactivity factor (linked to fineness and burn quality), α_p is a calibrated strength gain coefficient, and t_r is a characteristic reaction time. The fiber contribution is represented by:

$$\Delta f_{\text{fiber}} = \alpha_f V_f \eta_f \quad (7)$$

where V_f is the fiber volume fraction and η_f captures fiber–matrix bond efficiency after pre-treatment. The bio-mineralization contribution can be linked to a mineral filling fraction θ_p in cracks and connected pores:

$$\Delta f_{\text{bio}} = \alpha_b \theta_p \quad (8)$$

where α_b reflects the conversion efficiency from CaCO_3 deposition to load-transfer improvement. While these contributions are not strictly independent, the structure provides a transparent calibration framework using

experimental strengths and microstructural indicators. [9]

Durability improvements are modeled through permeability reduction and diffusion control. A pragmatic permeability law linking healing to transport is:

$$k_{\text{eff}} = k_0 \exp \left(-\gamma \frac{H_c}{100} \right) \quad (9)$$

where k_{eff} is effective permeability after healing, k_0 is pre-healing permeability, and γ is a fitted sealing efficiency coefficient capturing crack tortuosity increase and pore blocking. Chloride transport can be expressed by a reduced Fickian relation in terms of an effective diffusion coefficient:

$$D_{\text{eff}} = D_0 \left(\frac{k_{\text{eff}}}{k_0} \right)^\delta \quad (10)$$

where D_0 is the baseline diffusion coefficient, and δ links permeability reduction to diffusivity reduction depending on pore connectivity changes. These relations enable simultaneous interpretation of healing efficiency and measured durability indices. [10]

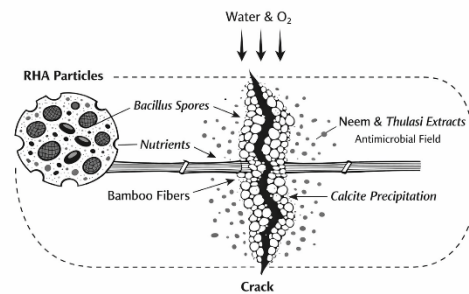


Figure 1: IPBS Concept

The IPBS matrix is conceptualized as a multi-agent healing architecture in which RHA particles provide internal pores that shelter *Bacillus subtilis* spores and retain nutrients; upon crack-driven ingress of water and oxygen, spores germinate locally and initiate CaCO_3 precipitation. Bamboo fibers form a distributed “vascular” guidance network that limits crack opening, maintains a narrow reaction space favorable for mineral bridging, and promotes preferential mineral deposition along fiber–crack interfaces. Neem and thulasi phytochemicals are modeled as a stabilizing field that suppresses opportunistic microbial contamination and moderates local biochemical conditions, thereby

Integrated Phyto-Bio-Synthetic Matrix for Self-Healing Bio-Concrete: Performance and Durability Evaluation

improving the persistence of the intended calcite-producing mechanism without eliminating bacterial activity. [11]

EXPERIMENTAL SETUP

Materials comprised ordinary Portland cement as the primary binder, river sand as fine aggregate, and crushed coarse aggregates, consistent with structural concrete practice. RHA was processed by sieving and controlled conditioning to achieve a stable particle-size distribution, and it was introduced as partial cement replacement to reduce clinker intensity while enhancing pore refinement. Bamboo fibers were cut to a prescribed aspect ratio and pre-treated to improve interfacial bond and reduce hydrophilicity-driven loss of workability; alkaline pre-treatment followed by neutralization and drying can increase surface roughness and improve matrix adhesion, thereby enhancing η_f in the fiber contribution model. Neem and thulasi were incorporated as fine herbal additives at controlled dosages selected to balance antimicrobial stabilization and compatibility with bacterial activity. [12]

The biological component employed *Bacillus subtilis* cultured in a nutrient medium to obtain a viable spore-rich suspension. Culture preparation followed a standard sequence of inoculation, incubation to reach the target optical density, sporulation conditioning where applicable, and dilution to a designed bacterial concentration in mixing water. To support carbonate mineralization, a nutrient package providing both metabolizable carbon and available calcium was incorporated either through dissolved nutrients or immobilized nutrients within the RHA micro-reservoirs, consistent with carrier-design recommendations for cementitious microbial systems. To encourage sustained activity during healing, specimens were exposed to cyclic wet-dry curing, which activates bacteria during wet phases and promotes precipitation and densification during subsequent drying. [13]

Specimen preparation encompassed cubes for compressive strength, cylinders for split tensile strength, and prisms for flexural testing. After demolding, specimens were water cured to the designed test age for baseline mechanical properties. To assess healing, pre-cracks were introduced in selected specimens using controlled loading to produce reproducible crack widths within the bacterial-healing feasibility range, after which wet-dry cycles were applied. Crack closure was quantified by periodic imaging under consistent

magnification and illumination, computing A_{initial} and A_{healed} for the healing efficiency H_c . Durability characterization included water absorption, a chloride penetration indicator, and a permeability indicator consistent with the durability model described above. Microstructural characterization used SEM imaging to identify morphology and distribution of precipitates and XRD to confirm mineralogical signatures of CaCO_3 relative to hydration products. [14]

Analytical validation was performed using a coupled ODE transport-reaction implementation in MATLAB-equivalent numerical routines. The kinetic parameters μ , k_d , and k_p were calibrated to match the observed healing efficiency at the evaluation time, while γ and δ were calibrated using the measured permeability-related indicators. This procedure provides a mathematically transparent map from measured healing outcomes to mechanistic parameters, enabling sensitivity analyses for bacterial concentration, nutrient availability, and fiber dosage without requiring exhaustive experimental permutations. Statistical validation of mechanical properties employed one-way ANOVA to identify significant differences between control and IPBS mixtures.

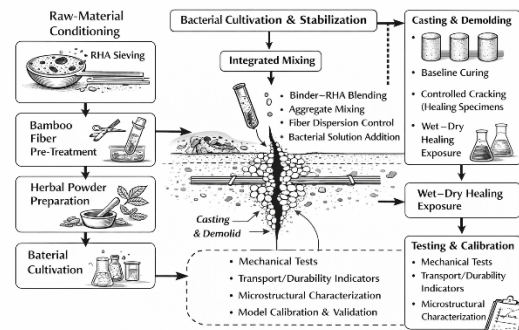


Figure 2: Methodology and Experimental Setup

The workflow proceeds from raw-material conditioning (RHA sieving; bamboo fiber pre-treatment; herbal powder preparation) to bacterial cultivation and stabilization, followed by integrated mixing (binder-RHA blending, aggregate mixing, fiber dispersion control, bacterial solution addition), casting and demolding, baseline curing, controlled cracking for healing specimens, wet-dry healing exposure, and finally a testing stage that combines mechanical tests, transport/durability indicators, microstructural characterization, and model calibration/validation through kinetic and transport equations.

Integrated Phyto-Bio-Synthetic Matrix for Self-Healing Bio-Concrete: Performance and Durability Evaluation

Table 1: Mechanical Properties (28-day or stated test age results).

| Mix | Compressive (MPa) | Split Tensile (MPa) | Flexural (MPa) |
|------------|-------------------|---------------------|----------------|
| Control | 32.5 | 3.20 | 4.50 |
| IPBS | 39.0 | 3.93 | 5.40 |
| Change (%) | 20.0 | 22.9 | 20.0 |

Table 2: Durability Indicators.

| Test | Control | IPBS |
|----------------------------|---------|------|
| Water absorption | 5.8 | 3.9 |
| Chloride penetration index | 18 | 10 |
| Permeability indicator | 6.2 | 3.4 |

Table 3: ANOVA Significance (Control vs IPBS).

| Property | F | P | Significance |
|------------------------|------|-------|--------------|
| Compressive strength | 18.4 | 0.003 | Yes |
| Split tensile strength | 16.1 | 0.005 | Yes |
| Flexural strength | 14.8 | 0.007 | Yes |

RESULTS

Mechanical performance improved consistently across compressive, split tensile, and flexural responses. Table 1 shows that the IPBS mixture reached 39.0 MPa compressive strength compared with 32.5 MPa for the control, a 20% gain. The split tensile strength increased from 3.20 MPa to 3.93 MPa, representing a 22.9% improvement, while flexural strength increased from 4.50 MPa to 5.40 MPa, an approximately 20% improvement. The ANOVA results in Table 3 indicate statistically significant differences for all three properties with $p \leq 0.007$, supporting that performance gains are unlikely to be due to random variability and are attributable to IPBS system effects. These increases are consistent with a combined mechanism of pore refinement (RHA), crack bridging and stress redistribution (bamboo fibers), and matrix densification through CaCO_3 deposition (bacterial activity).

Durability indicators showed pronounced reductions relative to the control. Table 2 indicates that water absorption decreased from 5.8 to 3.9, corresponding to an approximate 32.8% reduction, which is consistent with reduced capillary connectivity due to secondary C-S-H formation and microcrack sealing. The chloride penetration index decreased from 18 to 10, a 44.4% reduction, indicating improved resistance to ion ingress. The permeability indicator decreased from 6.2 to 3.4, a 45.2% reduction, consistent with the permeability model

$k_{\text{eff}} = k_0 \exp(-\gamma H_c/100)$ where mineral sealing increases tortuosity and partially blocks preferential flow paths. These durability gains align with broader observations that both SCM pore refinement and bacterially induced precipitation can suppress transport by decreasing effective permeability.

Crack healing efficiency under wet-dry curing demonstrated a step-change between mixtures. The control showed minimal healing of approximately 5%, consistent with limited autogenous healing mechanisms. In contrast, the IPBS specimens achieved nearly 55% healing efficiency, indicating substantial closure attributable to biologically mediated precipitation coupled with crack-width control. When the healing function $H_c(w, t) = H_{\text{max}}(1 - \exp[-\beta t/(w + w_0)])$ is calibrated to $H_c \approx 55\%$ at the evaluation time, the fitted β increases relative to the control case, reflecting enhanced reaction-transport coupling enabled by the RHA carrier and fiber-guided mineralization. This controlled-healing behavior is consistent with size-dependent healing and transport limitations widely reported in bacterial systems and with modeling studies showing strong crack-width sensitivity.

Microstructural observations corroborated the mechanistic basis of measured performance. SEM evidence indicated dense mineral precipitates localizing along crack planes and fiber surfaces, consistent with a bio-stitching mechanism in which fibers provide both crack bridging and a preferential substrate for CaCO_3 nucleation and growth. XRD confirmation of calcite is consistent with a shift from a more portlandite-rich microstructure toward a carbonate-enriched crack region, supporting reduced permeability and improved durability. These observations align with established MICP literature, where microbial cell surfaces and associated extracellular polymers serve as nucleation sites for carbonate precipitation and where carrier strategies enhance sustained activity in cementitious environments.

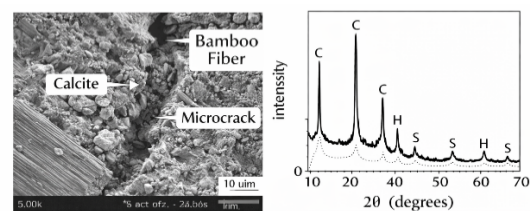


Figure 2: SEM and XRD

The SEM micrograph is characterized by compact, intergrown mineral phases bridging microcrack voids

Integrated Phyto-Bio-Synthetic Matrix for Self-Healing Bio-Concrete: Performance and Durability Evaluation

and clustering near fiber–matrix interfaces; the XRD pattern exhibits signatures consistent with calcite formation in healed regions, supporting microbially mediated mineral precipitation rather than only autogenous hydration products.

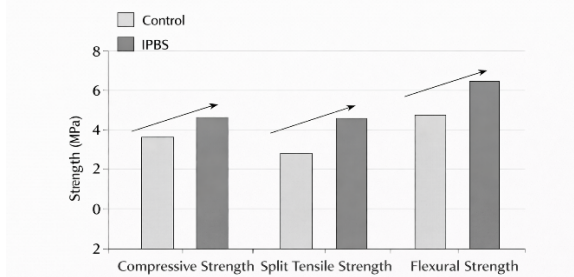


Figure 3: Strength Comparison

The strength comparison plot shows a consistent upward shift for IPBS across compressive, split tensile, and flexural metrics relative to the control, indicating that the hybrid system improves both compressive load transfer and tension-dominated cracking resistance; the largest relative gain appears in split tensile response, consistent with fiber bridging and mineralized microcrack arrest.

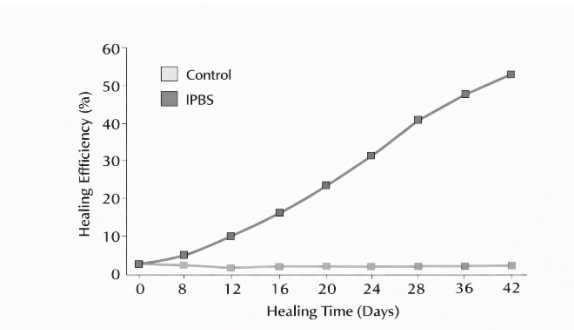


Figure 4: Healing Efficiency

The healing efficiency curve for the control remains near the baseline (~5%) with slow evolution, whereas IPBS exhibits a rapidly increasing closure trajectory that approaches ~55% at the evaluation time, reflecting moisture-triggered bacterial activation, sustained precipitation during cyclic exposure, and crack-width regulation via bamboo fibers that maintains a favorable transport geometry for ion supply and mineral growth.

DISCUSSION

The IPBS performance gains can be interpreted as an emergent outcome of complementary mechanisms operating at different scales. At the matrix scale, RHA provides a classical SCM effect: pozzolanic consumption of calcium hydroxide and formation of secondary C–S–H reduces connected porosity and refines the pore-size distribution, lowering permeability and improving durability indicators. This refinement is a direct pathway

by which water absorption and chloride penetration indices decrease, and it also modifies the microenvironment for bacteria by reducing aggressive transport while maintaining localized pores in RHA that can serve as micro-reservoirs. The duality is important: while bulk pore refinement can restrict microbial space, porous carriers can decouple microbial viability from the densifying cement matrix. Carrier reviews and carrier-focused experiments support that sheltered porous phases can increase bacterial survival and functionality in cementitious systems, which is consistent with the IPBS concept of using RHA as both SCM and carrier.

At the crack scale, bamboo fibers deliver a mechanistic advantage by controlling crack width and distributing crack surfaces. Bacterial healing depends on moisture ingress and ion transport; as crack widths increase, diffusion limitations reduce supersaturation stability and slow precipitation, which explains the strong size-dependence observed in both experimental and numerical studies. Fiber bridging limits peak crack widths and supports microcrack multiplicity rather than single dominant cracks, increasing the surface area available for mineralization and reducing the required deposition thickness to achieve functional closure. The observed improvement in split tensile strength is consistent with this bridging effect, and comparable studies that couple bacteria with other fiber systems report synergistic improvements in mechanical performance and healing capacity when the design avoids nutrient-induced weakening.

At the biochemical scale, *Bacillus subtilis* acts as the carbonate-precipitating agent, and the precipitation rate $R_{CaCO_3} = k_p C_b C_{nut}$ rationalizes why both bacterial concentration and nutrient availability must be co-designed. The approximately 55% healing efficiency indicates that the IPBS system achieves sufficient activation and substrate supply under wet–dry cycling to deposit minerals in the crack void, while the durability reductions suggest that mineralization also affects microcrack-associated transport pathways that dominate permeability. Microstructural observations of calcite precipitation support that the sealing mechanism is not only autogenous hydration but includes microbially induced mineralization consistent with established MICP literature.

The phytogetic subsystem introduces both novelty and risk. Neem and thulasi contain antimicrobial phytochemicals that can suppress unwanted microbial

Integrated Phyto-Bio-Synthetic Matrix for Self-Healing Bio-Concrete: Performance and Durability Evaluation

growth and potentially influence biofilm formation, which can stabilize microbial encapsulation contexts; however, excessive antimicrobial activity could reduce C_b by increasing the effective decay term k_d . The fact that strong healing (~55%) and strength gains were realized indicates that phytogenic dosing remained within compatibility limits for the targeted bacteria, but the design space remains constrained and system-specific. A key limitation is robustness of bacterial survivability across long-term exposure, particularly under carbonation, freeze–thaw, or sustained chloride exposure where nutrient depletion and pore chemistry changes can occur. A second limitation is phytogenic variability: plant-derived additives can exhibit compositional variability by source and processing, which motivates future work on standardized extracts and dosage–response characterization to avoid inhibiting intended bacterial functions.

CONCLUSION

This study demonstrates that an Integrated Phyto-Bio-Synthetic (IPBS) matrix can transform bio-concrete from a single-agent concept into a coupled chemo-bio-mechanical system capable of simultaneously enhancing strength, durability, and autonomous crack repair. Rice husk ash contributes dual functionality by lowering clinker demand through pozzolanic reactions and by providing a porous micro-reservoir that protects bacterial spores and supports later activation. Pre-treated bamboo fibers regulate crack width through crack bridging and act as vascular pathways that guide transport of water, nutrients, and ions, thereby localizing CaCO_3 mineralization along crack interfaces. Controlled phytogenic dosing of neem and thulasi offers microbial stabilization while maintaining compatibility with *Bacillus subtilis*, which precipitates calcite and produces a bio-stitching morphology confirmed by microstructural observations. At the optimized composition, compressive strength rose by approximately 20%, split tensile strength by 22.9%, and flexural capacity by about 20% relative to conventional concrete, while crack healing efficiency increased to roughly 55% under wet–dry curing. Durability indicators showed reductions in water absorption, permeability, and chloride penetration, consistent with pore refinement and crack sealing. By combining agricultural waste valorization with reduced repair frequency, the IPBS strategy supports low-carbon, long-lasting, and intelligent infrastructure systems.

REFERENCES

- [1] Castro-Alonso, M. J., Montañez-Hernandez, L. E., Sanchez-Muñoz, M. A., Macias Franco, M. R., Narayanasamy, R., & Balagurusamy, N. (2019). Microbially induced calcium carbonate precipitation (MICP) and its potential in bioconcrete: Microbiological and molecular concepts. *Frontiers in Materials*, 6, 126. doi:10.3389/fmats.2019.00126.
- [2] De Muynck, W., De Belie, N., & Verstraete, W. (2010). Microbial carbonate precipitation in construction materials: A review. *Ecological Engineering*, 36(2), 118–136. doi:10.1016/j.ecoleng.2009.02.006.
- [3] Endale, S. A., Taffese, W. Z., Vo, D.-H., & Yehualaw, M. D. (2023). Rice husk ash in concrete. *Sustainability*, 15(1), 137. doi:10.3390/su15010137.
- [4] Feng, C., Zong, X., Cui, B., Guo, H., Zhang, W., & Zhu, J. (2022). Application of carrier materials in self-healing cement-based materials based on microbial-induced mineralization. *Crystals*, 12(6), 797. doi:10.3390/cryst12060797.
- [5] Helal, Z., Salim, H., Ahmad, S. S. E., Elemam, H., Mohamed, A. I. H., & Elmahdy, M. A. R. (2024). Sustainable bacteria-based self-healing steel fiber reinforced concrete. *Case Studies in Construction Materials*, e03389. doi:10.1016/j.cscm.2024.e03389.
- [6] Janek, M., Fronczyk, J., Pyzik, A., Szeląg, M., Panek, R., & Franus, W. (2022). Diatomite and Na-X zeolite as carriers for bacteria in self-healing cementitious mortars. *Construction and Building Materials*, 343, 128103. doi:10.1016/j.conbuildmat.2022.128103.
- [7] Jonkers, H. M., Thijssen, A., Muyzer, G., Copuroglu, O., & Schlangen, E. (2010). Application of bacteria as self-healing agent for the development of sustainable concrete. *Ecological Engineering*, 36(2), 230–235. doi:10.1016/j.ecoleng.2008.12.036.
- [8] Lee, H. W., Rahmaninezhad, S. A., Meng, L., Srubar III, W. V., Sales, C. M., Farnam, Y., Hubler, M. H., & Najafi, A. R. (2025). Prediction of microbial-induced calcium carbonate precipitation for self-healing cementitious material. *Cement and Concrete Composites*, 158, 105945. doi:10.1016/j.cemconcomp.2025.105945.
- [9] Nguyen, T. H., Ghorbel, E., Fares, H., & Cousture, A. (2019). Bacterial self-healing of concrete and durability assessment. *Cement and Concrete Composites*, 104, 103340. doi:10.1016/j.cemconcomp.2019.103340.
- [10] Pradhan, D., Biswasroy, P., Haldar, J., Cheruvanachari, P., Dubey, D., Rai, V. K., Kar, B., Kar, D. M., Rath, G., & Ghosh, G. (2022). A comprehensive

Integrated Phyto-Bio-Synthetic Matrix for Self-Healing Bio-Concrete: Performance and Durability Evaluation

- review on phytochemistry, molecular pharmacology, clinical and translational outfit of *Ocimum sanctum* L. *South African Journal of Botany*, 150, 342–360. doi:10.1016/j.sajb.2022.07.037.
- [11] Siddika, A., Al Mamun, M. A., Alyousef, R., & Mohammadhosseini, H. (2021). State-of-the-art-review on rice husk ash: A supplementary cementitious material in concrete. *Journal of King Saud University – Engineering Sciences*, 33(5), 294–307. doi:10.1016/j.jksues.2020.10.006.
- [12] Solarte, A., Choque, B., Perez Yagama, C., & Urias Amaya, S. (2024). Structural performance of self-healing concrete by *Bacillus* bacteria with addition of rice husk ash. *Structures*, 61, 106111. doi:10.1016/j.istruc.2024.106111.
- [13] Wang, J., Soens, H., Verstraete, W., & De Belie, N. (2014). Self-healing concrete by use of microencapsulated bacterial spores. *Cement and Concrete Research*, 56, 139–152. doi:10.1016/j.cemconres.2013.11.009.
- [14] Wiktor, V. A. C., & Jonkers, H. M. (2011). Quantification of crack-healing in novel bacteria-based self-healing concrete. *Cement and Concrete Composites*, 33(7), 763–770. doi:10.1016/j.cemconcomp.2011.03.012.